Available online www.worldscientificnews.com

World Scientific News

An International Scientific Journal

WSN 216 (2026) 1-19 EISSN 2392-2192

Reinforcing Silica Fume and Kaolin with Alumina (Al_2O_3) and Aluminum Fluoride Trihydrate ($AlF3.3H_2O$) for the Synthesis of Mullite Refractories

S. Kamara. [1,2*]

1. Department of Chemical Engineering, School of Water and Environment, Chang'an University, Xi'an 710054, China; ksaidu2013@gmail.com (SK)
2. Department of Engineering, Faculty of Engineering and Technology, Ernest Bai Koroma University of Science and Technology, Magburaka Campus, Sierra Leone, ksaidu2013@gmail.com, saiduk@ebkustsl.edu.sl

* Correspondence: ksaidu2013@gmail.com, saiduk@ebkustsl.edu.sl

https://doi.org/10.65770/IBDQ6493

ABSTRACT

Refractories are well-known ceramics of chemical compositions such as $Al2O_3$, SiO_2, MgO, etc. Various methods or routes are employed to fabricate refractory materials. Solid-state sintering is the most common and suitable method utilized to fabricate refractories in the laboratory and on a commercial scale. Two experiments were conducted using different raw materials and different stoichiometric quantities. In this research, silica fume (SiO_2 > 99%), kaolin ($Al_2Si_2O_5(OH)_4$ and alumina (Al_2O_3) were utilized. Silica and kaolin are solid waste materials used as starting materials for synthesizing mullite refractory ceramics. Aluminum fluoride trihydrate was added to the appropriate reacting mixtures to aid the ceramic or refractory formation. 10g of Al_2O_3 and 4g of SiO_2 were measured in the first experiment, while 10.2g of Al_2O_3 and 12.9g of $Al_2Si_2O_5(OH)_4$ measured in the second experiment. Three specimens were prepared from each of the two sets of prepared mixtures and heated at 1000^0C. 1100^0C, and 1200^0C in the muffle furnace. The specimens were ground into powder form to make them ready for characterization. SEM, XRD, EDS, and FTIR characterizations were done on the specimens to determine the morphology, crystallinity, chemical compositions, functional groups, and absorption frequencies in the fabricated composites.

Keywords: experiment, silica, kaolin, mullite, temperature, characterization

(Received 12 April 2026; Accepted 15 May 2026; Date of Publication 7 June 2026)

1. INTRODUCTION

Refractories are ceramic materials that can endure extremely high temperatures and provide insulation eg, mullite, alumina, zirconia, magnesia, silicon carbide, etc. [1-3]. Their properties are versatile in both ceramic and refractory industries for various engineering applications. The popular industries for marketing refractories are chemical, petrochemical, industrial heating process, power generation, and heavy industrial processing industries [4-6].

Composite refractories are not well-known on a commercial scale [7]. They are prepared by either conventional (traditional) or chemical methods [8]. The conventional method involves sintering the aluminosilicate samples at high temperatures [9-11]. Commercial quantities of refractory composites are nowadays fabricated in the laboratory through solid-state sintering reactions, which involve cost-effective starting materials [12-18].

Many researchers have reported the use of MgO as an additive to enhance the use of refractories in various applications. The utilization of MgO and $AlF_3.3H_2O$[17, 19] in the synthesis of composite refractories from silica is promising due to their production cost and easy availability. The powdered silica is normally mixed with water and other materials to form a paste during the fabrication of ceramics. Many sources (fly ash, rice husk, demolition wastes, blast furnace slag, volcanic ash, etc.) of Al and Si have been investigated in many studies. Silica is a cost-effective, finely powdered, and dark-shaded material**.** Kaolin is a light-shaded and more costly mineral than silica. This work outlines two experiments with different raw materials and an additive. The raw materials used in the two experiments are SiO_2, $Al_2Si_2O_5(OH)_4$, and Al_2O_3, with $AlF_3.3H_2O$ as an additive [17, 19]. The main focus of this work was to study refractory composites synthesized from silica and kaolin and make a comparative analysis of all products in the two experiments. Characterization techniques are done to determine the morphologies, crystallinity, chemical components, functional groups, etc. of experimental samples. It has been reported that the main refractory products identified in experimental analysis involving silica and kaolin are cordierite, mullite, and kyanite, proving their suitability as raw materials [20-22]. The properties of silica are super refractory and can therefore be employed as an alternative, inexpensive raw material to the conventionally used alumina.

The process by which the particles in a refractory material bond together when fired at a regulated temperature is called sintering. The material needs sufficient firing to avoid breakage even when it comes in contact with water. Refractory materials are heat-resistant, non-metallic, inorganic materials with suitable physical and chemical stability when subjected to environments with extreme temperatures [14, 23-25] such as in industrial vessels and furnace linings where cement, metals, glass, etc are manufactured, ranging between 600^0C to 2000^0C. The properties of refractory materials in industrial applications are thermal stress/strain, mechanical abrasion, and corrosion/erosion resistance from molten solids, hot liquids, and gases [26, 27]. The refractory industry is essential to other manufacturing industries because other production activities would not be accomplished in its absence.

The classification of refractory materials depends on their chemical components and forms, such as Al_2O_3, MgO, SiO_2, CaO, ZrO_2, and Cr_2O_3, and their combinations. The fabricated refractories can either be shaped or unshaped. The shaped refractories are formed by mixing, shaping, and firing. Conventional refractories have poor corrosion resistance and penetration, particularly in the basic environment, and structural fragmentation [28-30], but the issues were resolved decades ago by adding carbon to oxide-based refractory products. Carbon is known to have high thermal conductivity, low thermal expansion coefficient, and non-wettability [31-35].

Refractory products made of carbon have improved physical and chemical properties than those products whose oxides are free of carbon [36, 37]. Carbon-based refractories are more sustainable and can be used for a lifetime in industrial furnace linings.

Among the refractories present, the mullite crystalline phase of calcined reactive alumina is more pronounced, with better microstructure, because of its small grain size, purity, and homogeneous mixture of the clays [22, 38-40]. According to three Indian researchers (Neyveli, Panruti, and Udayarpalayam), the high loss of water in boehmite samples results in surface cracks and poor strength [11, 41, 42]. Aksay et.[43], reported that the main problem encountered in conventional processing methods is the presence of high impurities in the final products, and this can be prevented by the use of highly purified Si Al [44-46]. Hydrated aluminum hydroxide and silicon dioxide calcined at 1300^0C result in the formation of orthorhombic mullite. Refractory materials can be sintered, fused, or chemically based on the method of preparation [47-50]. Fused mullite is formed when the raw material is melted in an electric furnace, while powdered chemical mullite is formed by some techniques referred to as sol-gel, co-precipitation, hydrolysis, spray hydrolysis, and chemical vapor deposition [42, 51-53].

2. EXPERIMENTAL METHOD

2.1. Aim

In general, this work was carried out to investigate refractory materials fabricated from silica fume, kaolin reinforced with $AlF_3.3H_2O$, using SEM, EDS, FTIR, and XRD characterization techniques to determine the crystalline, chemical compositions and absorption frequencies of functional compounds in the fabricated ceramic materials.

2.2. Materials

The materials involved in this experimental research are aluminum oxide (Al_2O_3), silica (SiO_2), kaolin ($Al_2Si_2O_5(OH)_4$, and aluminum fluoride trihydrate ($AlF_3.3H_2O$). The silica ($SiO_2 > 99\%$) was purchased from Xi'an Linyuan Silica Limited, Shaanxi Province, while alumina and aluminum fluoride trihydrate are reserved laboratory chemicals for research purposes.

2.3. Instruments

Analytical electronic balance, weighing papers, grinding mill, E-ZIRCON hydraulic press jack, thermostatic drier, muffle furnace (1300 ℃ maximum heating capacity), scanning electron microscope (SEM), x-ray diffraction (XRD), energy dispersion x-ray spectroscopy (EDS), Fourier transform infrared (FTIR), and jade 6 and Origin 9 software [17].

2.4. Processing and Procedures

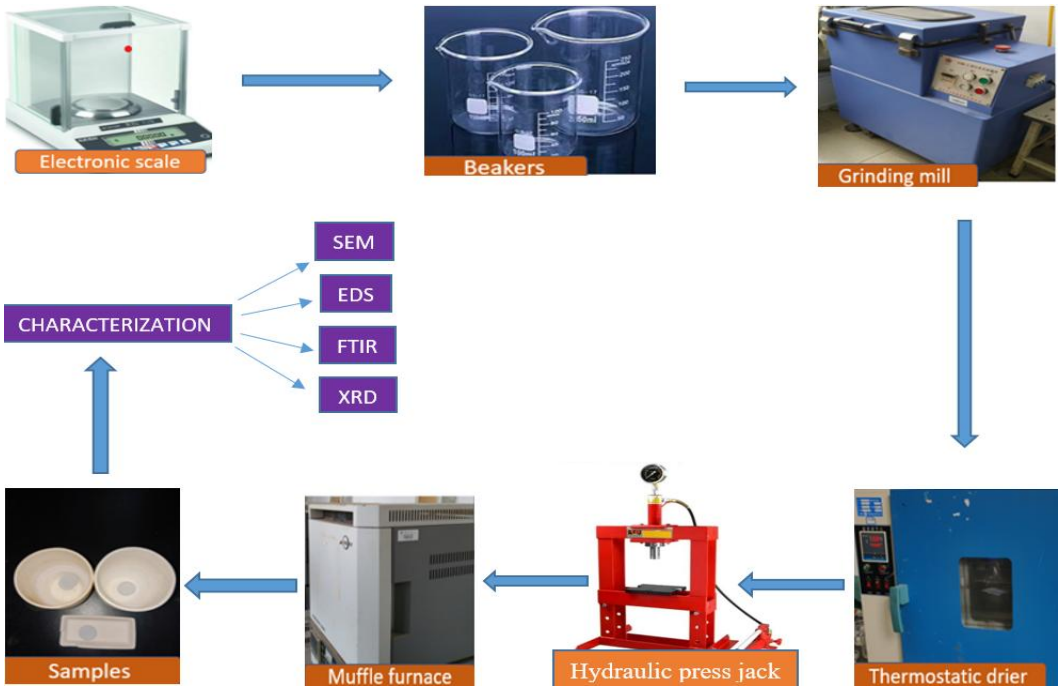

Figure 1. Illustration of instrumental setup for sample preparation.

Figure 1 is a display of the instrumental setup for sample processing. Refractory materials were synthesized by conducting two different experiments with different starting materials labeled 1 and 2. The three starting materials (Al_2O_3, SiO_2, and $Al_2Si_2O_5(OH)_4$) were processed and secured first (10g, 4g) and second (10.2g, 12.9g) weight values. In experiment one (1), 10g of Al_2O_3 and 4g of SiO_2 were combined, and then added 1g of $AlF_3.3H_2O$ as an additive. Experiment two (2) was also demonstrated by mixing 10.2g of Al_2O_3 and 12.9g of $Al_2Si_2O_5(OH)_4$ with 2g of $AlF3._3H_2O$ additive.

Three sets of specimens labeled A, B, and C were prepared from each of the two experimental mixtures. The three specimens were placed in a grinding mill for further mixing for 10 minutes. The samples are removed from the grinding mill after mixing and placed in a thermostatic drier for about 2 to 3 hours at a regulated temperature of 60^0C °C to remove the moisture content. The specimens were then molded into round-shaped objects using an EZIRCON hydraulic press jack before being fired into a muffle furnace that has a maximum heating capacity of 1300^0C. In the muffle furnace, the three specimens were sintered at 1000^0C, 1100^0C, and 1200^0C at a constant temperature rate of 10^0C per minute for 4 hours. Remove the samples from the furnace and make them ready (granulated and powdered) for characterization. This process and procedure are the same for both experiments 1 and but with different reacting materials. Three characterization techniques (XRD, EDS, and FTIR) were used for this research. The XRD was utilized to identify the presence of the crystalline phases in the sintered specimens. The EDS was employed to determine and measure the chemical components of the specimens, while the FTIR was utilized to identify the different functional groups present in the prepared specimens. The EDS tool is operated by the SEM machine. The functional groups of the samples were determined by FTIR (Nicolet 5700, Thermo, America) in the wavenumber range $4500cm^{-1}$ – $500cm^{-1}$.

3. RESULTS AND DISCUSSION

3.1. Analysis of Samples Prepared From Silica Fume

3.1.1. Scanning Electron Microscope (SEM)

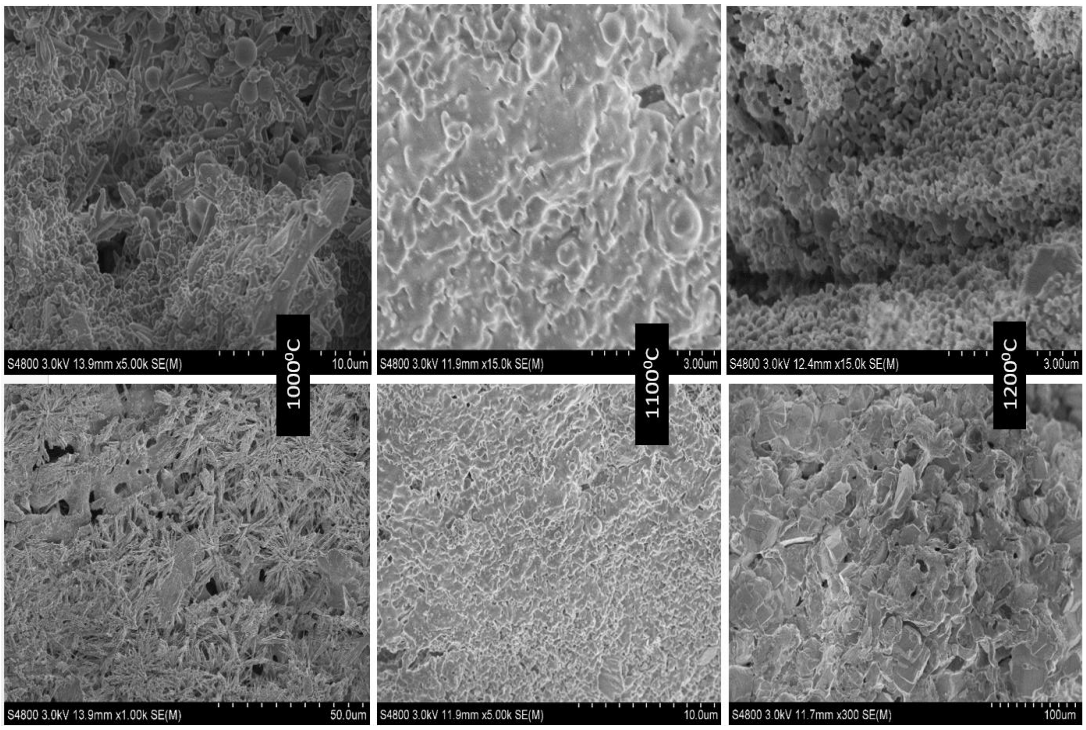

Figure 2. SEM micrographs of mullite samples sintered at 1000^0C, 1100^0C, and 1200^0C

The SEM images in **Figure 2** above show the micrographs of mullite samples between 1000^0C to 1200^0C. The samples were magnified at various resolutions ranging from 3 µm to 100 µm. The crystalline phases in the micrographs are mullite, kyanite, corundum, quartz, and monganite, with mullite and kyanite ceramics being the major phases. According to the SEM results above, the morphology of the microstructures does not show a significant difference in the sintered samples. The tiny crystals of mullite are seen to be randomly distributed in the micrographs of the three samples. The clustered, elongated, glassy-like grains and the bubble-like secondary mullite are observed across the micrographs of the three samples. It has been observed that mullite grain size increases with an increase in temperature, and the mechanism is known as dissolution precipitation.

3.1.2. Energy Dispersion X-Ray Spectroscopy (EDS)

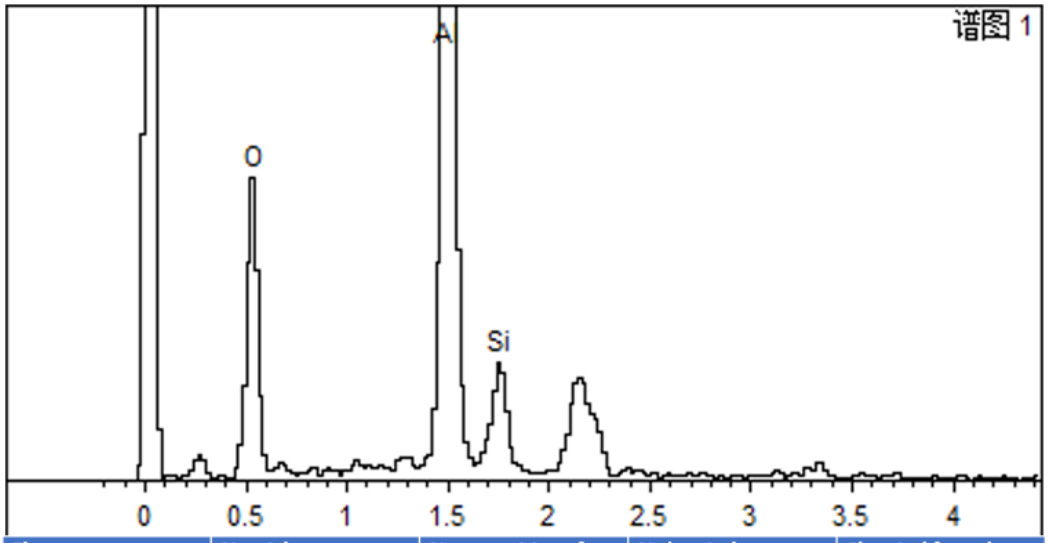

Element	% weight	% composition of atom	% chemical composition	Chemical formula
Al	43.16	32.51	81.55	Al_2O_3
Si	8.62	6.24	18.45	SiO_2
O	48.21	61.25	-	-
Total	100.00	100.00	100.00	

Figure 3. EDS spectrum and table for a selected silica fume sample.

The EDS results above (**Figure 3**) show Al, Si, and O as the constituent elements in the sample. Silica and alumina are the two main chemical compounds shown by the EDS results. AlF3.3H2O was used as an additive to the reacting materials, but was not identified according to the EDS result above. This is probably because lighter elements or materials are not normally detected by the EDS. The percentage composition of Al_2O_3 is 81.55% while SiO_2 is 18.45%. Silica and alumina were the materials used to prepare the sample, using a minute quantity of aluminum fluoride trihydrate as an additive. $AlF_3.3H_2O$ lowers the melting point below 1000^0C and improves the conductivity of a material. The percentage weights and compositions of the elements are explained in Figures 4 and 5 below.

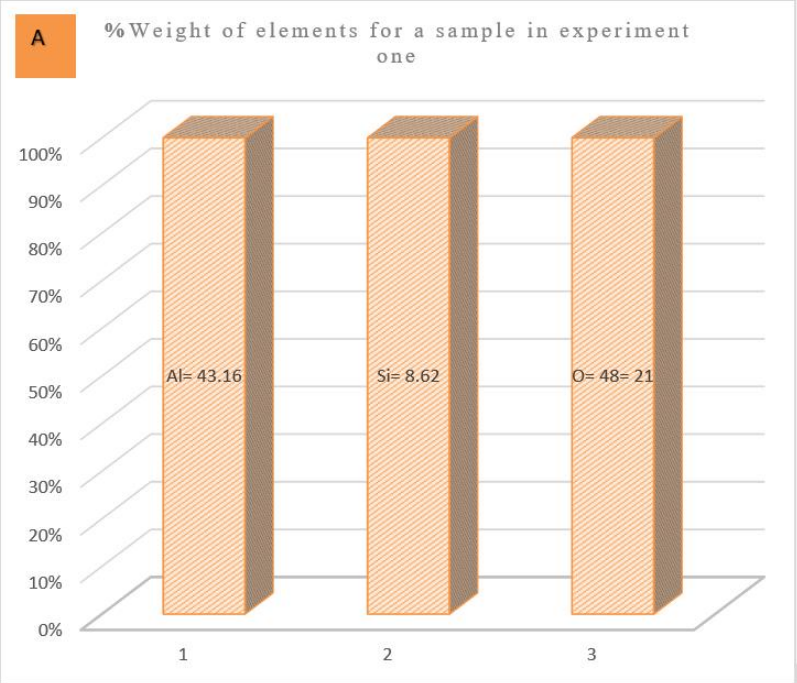

Figure 4. Percentage weights of elements for a selected silica sample.

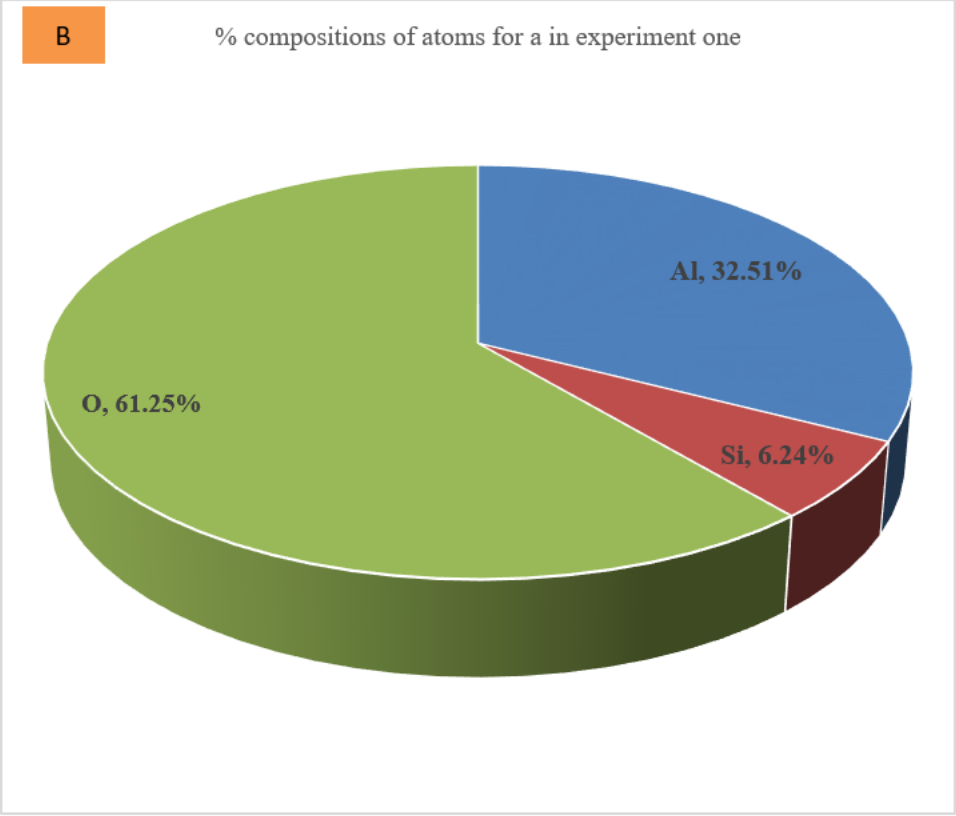

Figure 5. Percentage compositions of atoms for a selected silica sample.

According to **Figures 4 and 5** above, the percentage weights and compositions of Al are 43.16% and 32.51% respectively. The weight of Si is 8.21% with a composition of 6.24% while O has 48.21% and 61.25% weight and compositions respectively.

3.1.3. Fourier Transform Spectroscopy (FTIR)

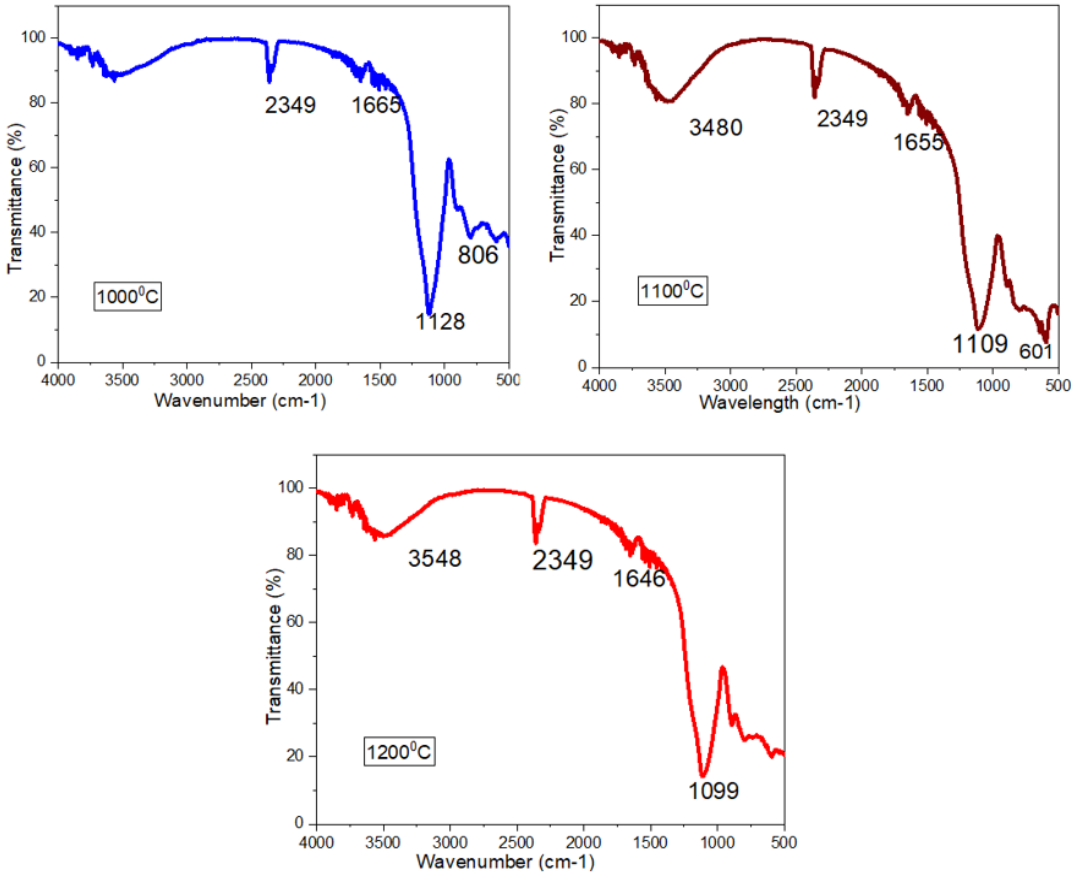

Figure 6. FTIR spectra for samples prepared from silica fume.

The FTIR of **Figure 6** above shows the three samples experiment one sintered at 1000^0C, 1100^0C, and 1200^0C. They have absorption bands with wavenumbers of 2349 cm^{-1}, 1665$cm^{-1,}$ 1128$cm^{-1,}$ and 806cm^{-1} for samples sintered at 1000^0C. The sample sintered at 1100^0C has wavenumbers of 3480cm^{-1}, 2349cm^{-1}, 1656cm^{-1}, and 1109cm^{-1}. The wavenumbers observed in the third sample are 3548cm^{-1}, 2349cm^{-1}, 1646$cm^{-1,}$ and 1099cm^{-1}. According to the FTIR spectra above, the wavenumber 2349cm^{-1} observed in all three sintered samples depicts the O=C=O stretching functional group of the carbon dioxide compound. The FTIR data for the samples in experiment one indicate the strong appearance of O=C=O bending in all three samples. The wavenumbers 1099 and 1089 show the appearance of Si-O-Si stretching.

3.1.4. XRD

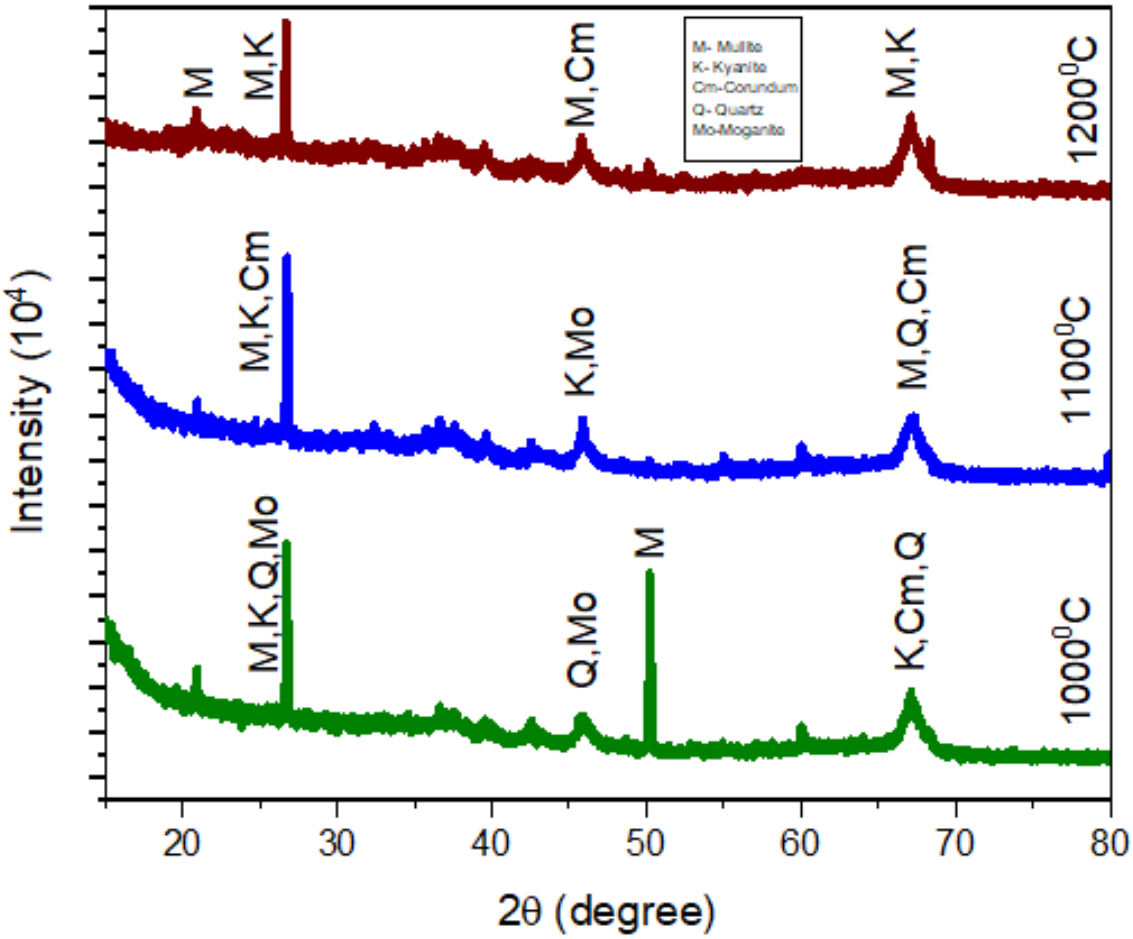

Figure 7. XRD spectrum for samples from silica fume.

The XRD result in **Figure 7** shows the phases of seven crystalline structures (mullite, kyanite, corundum, quartz, and moganite) formed in the three sintered samples. The formation of refractory crystals increases as the sintering temperature increases from 1000^0C to 1200^0C. Analysis of the above spectrum indicates that mullite and kyanite are discovered as the main refractory composite synthesized in this experiment. The evolution of both refractory composites begins at $2\Theta=26.8^0$ with an intensity (I)=279.4 and its formation occurs along the same plane of 2Θ in the first, second, and third samples. The fabrication of kyanite in this experiment is unprecedented and phenomenal, and this shows a marked difference from those crystalline materials fabricated in the parallel experiment that involves kaolin as raw material, from which mullite is the main refractory product, along with other crystalline phases. It has been reported that kyanite crystals can be converted to mullite when calcined above 1250^0C [17]. The effect of temperature increase on the formation of mullite and kyanite composites does not show a significant difference across the three samples.

3.2. Analysis of Samples Prepared from Kaolin

3.2.1. Scanning Electron Microscope (SEM)

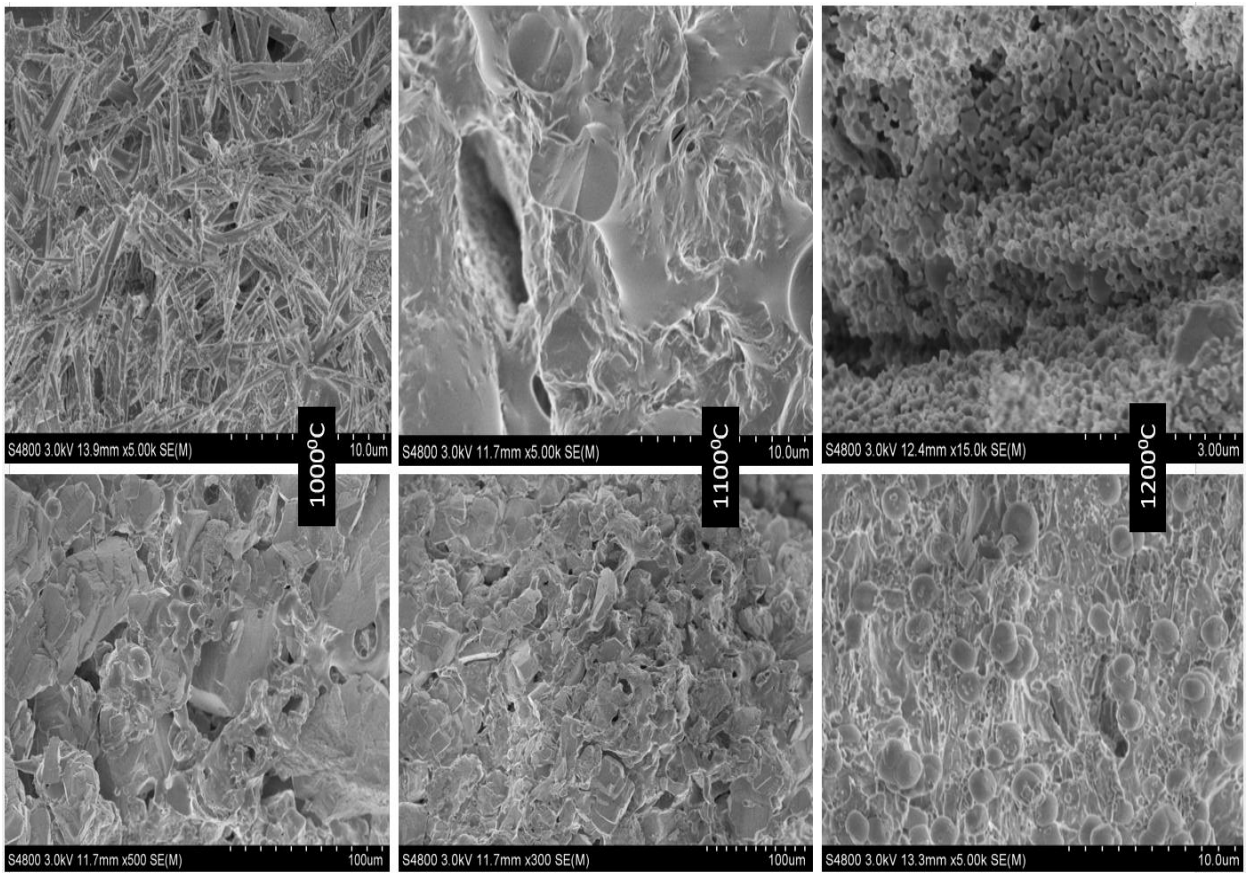

Figure 8. SEM micrographs of mullite samples sintered at 1000^0C, 1100^0C, and 1200^0C.

Figure 8 above shows the SEM images of mullite samples sintered at 1000^0C, 1100^0C, and 1200^0C and magnified at various resolutions. Mullite, corundum, alumina, and quartz are the main crystalline phases. The granular agglomerates in the microstructure are observed to be glassy, elongated, and bubble-like. The clustered, lengthened grains in the sample fired at 1000^0C with a magnification of 10 µm form the primary mullite. The scaly and bubble-like grains form the crystals' secondary mullite phase at higher temperatures.

3.2.2. Energy Dispersion X-Ray Spectroscopy (EDS)

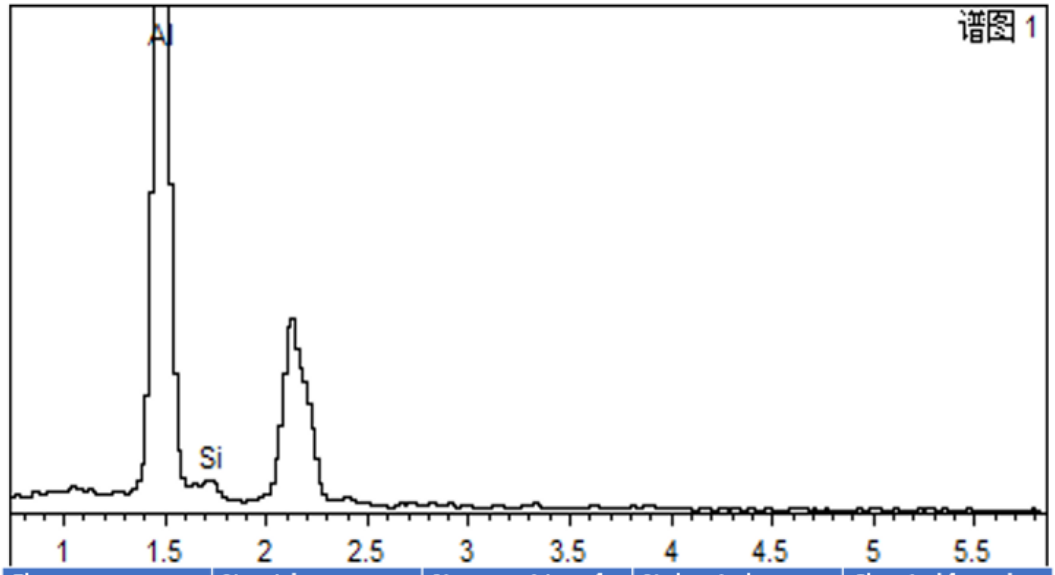

Element	% weight	% composition of atom	% chemical composition	Chemical formula
Al	51.71	39.07	97.71	Al_2O_3
Si	1.07	0.78	2.29	SiO_2
O	47.22	60.16		
Total	100.00	100.00	100.00	

Figure 9. EDS spectrum and table for a selected sample prepared from kaolin.

Figure 9 above shows the EDS results of the samples in experiment two. It has the same constituent elements as those in experiment one. The major chemical compound identified in the experimental sample (**Figure 9**) is alumina, while silica is minor. Al_2O_3 and $Al_2Si_2O_5(OH)_5$ are the materials used to prepare the sample under investigation. The percentage weight and composition of Al in the sample are 51.71% and 39.07% respectively, while the weight and composition of Si are 1.07% and 0.78% respectively. The percentage weights and compositions for a sample in experiment two are represented in **Figures 10 & 11** below.

Figure 10. Percentage weights of elements for a selected sample prepared from kaolin.

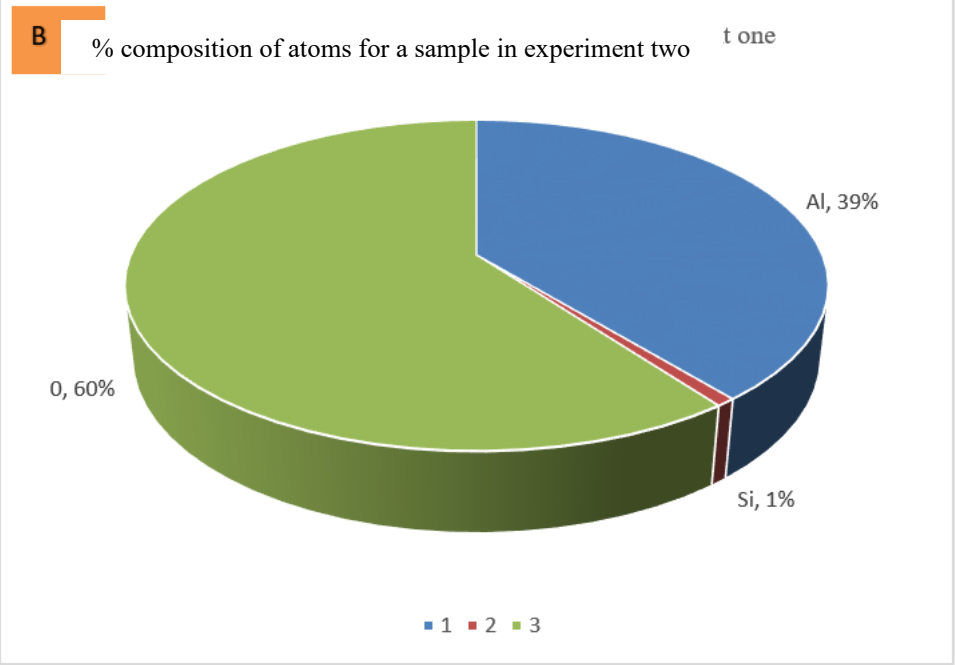

Figure 11. Percentage compositions of atoms for a selected sample prepared from kaolin.

$AlF_3.3H_2O$ is used as an additive in both experiments two. Comparatively, it is observed that the percentage compositions of Al_2O_3 in both experiments 1 and 2 are higher than those of SiO_2. The analysis further reveals that the percentage composition of SiO_2 in experiment two is far less than that shown in one. This is probably because the silica fume is composed of a higher content of SiO_2 than kaolin.

In summarizing the EDS analysis of the two experimental samples, it is observed that Al_2O_3 and Al show higher percentage weights and compositions for the sample in experiment two, which involved kaolin and alumina, than those in experiment one, in which silica and alumina were utilized. This is probably because the kaolin used as the starting material is an alumina silicate compound as opposed to silica ash which is 99% pure silica material. The compositions Al_2O_3 and Al in experiment two are 97.71% and 39.07% respectively.

It is further noted that the amounts of SiO_2 and Si for samples in one surpass those in two. The silica ash used as a starting material is purely SiO_2. In experiment one, the SiO_2 and Si have compositions of 18.45% and 6.24% respectively. The chemical compositions in both experiments involving silica and kaolin as raw materials successfully led to the synthesis of refractory ceramics. Alumina and silica are important components in the refractory industry.

3.2.3. Fourier Transform Spectroscopy (FTIR)

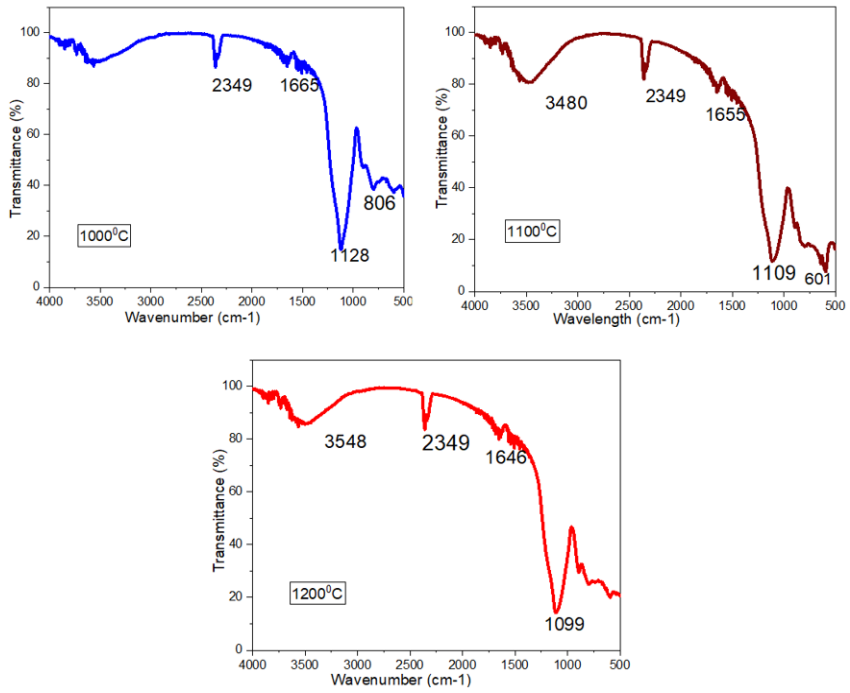

Figure 12. FTIR spectra for samples prepared from kaolin.

In **Figure 12** above, the FTIR data for the three samples in experiment two also indicate the strong appearance of O=C=O bending in all three samples in the same way as those in experiment one. The wavenumbers 1099cm^{-1} and 1089cm^{-1} show the appearance of Si-O-Si stretching. Based on the analysis of all FTIR experimental results, it is observed that O=C=O and Si-O-Si stretching vibrations are typical in all four experiments. Based on all the FTIR experimental results, it is observed that O=C=O and Si-O-Si stretching vibrations are typical in both two experiments.

3.2.4. XRD

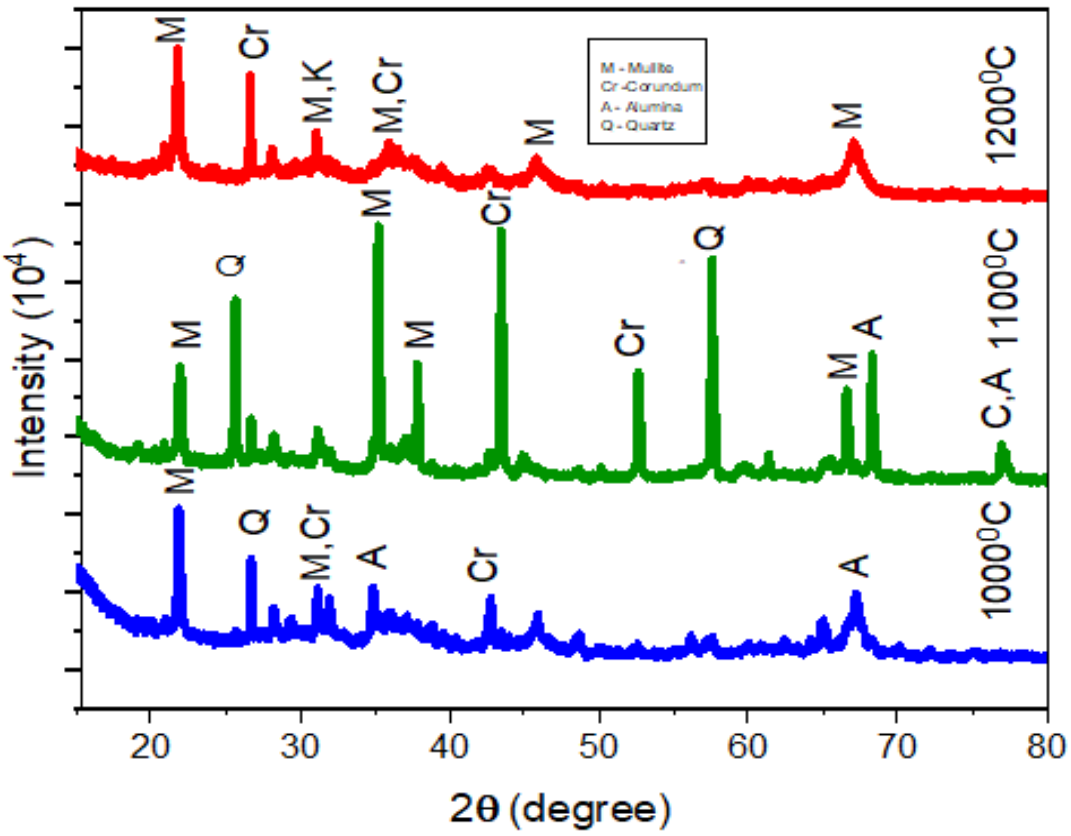

Figure 13. XRD spectrum for samples from kaolin.

The spectrum in **Figure 13** shows the evolution of four phases of crystalline materials in the specimens. Mullite was identified in samples A, B, and C sintered at 1000^0C, 1100^0C, and 1200^0C according to the above result. The number of mullite crystals formed increased when the sample was sintered at a higher temperature of 1200^0C. The formation of mullite crystals starts at $2\Theta = 21.8^0$ with an intensity (I) = 259.9 and the pattern of formation of these refractory materials is observed along similar planes of 2Θ in all three samples. Several crystalline structures are observed across the various temperatures of the three samples in experiment one which can be linked to the addition of $AlF_3.3H_2O$ as an additive to the mixture of kaolin ($Al_2Si_2O_5(OH)_4$) and alumina (Al_2O_3) starting materials [17].

4. CONCLUSION

Solid-state sintering was used to fabricate mullite refractory materials from silica fume and kaolin in two different tests. The EDS results in experiments 1 and 2 show that Al, Si, and O are present in the fabricated ceramic materials. It further reveals the percentage compositions of Al_2O_3 and SiO_2 in the synthesized refractory materials. On the other hand, the FTIR analysis in experiments 1 and 2 reveals the absorption frequencies of the Si-O-Si and O=C=O functional groups. Analysis of the XRD results in both experiments clearly shows the evolution of mullite ceramics. Kyanite is observed alongside mullite ceramics in the XRD spectrum in **Figure 7**. According to the analysis, the evolution of the mullite increases with an increase in temperature. Solid waste with significant aluminosilicate content can be used as a cost-effective raw material for the synthesis of ceramic materials.

Funding: This work was supported by the National Natural Science Foundation of China.

Acknowledgments: Thanks to the School of Water Resources and Environment, Chang'an University, and the Faculty of Engineering and Technology, Ernest Bai Koroma University of Science and Technology, for providing the platform to carry out this research successfully.

Conflicts of Interest: The authors declare no conflict of interest.

References

[1] P. Sengupta and P. Sengupta, "Manufacturing and properties of refractories," *Refractories for the Chemical Industries,* pp. 43-84, 2020 http://dx.doi.org/10.1007/978-3-030-61240-5_3.

[2] S. Biswas, D. Sarkar, S. Biswas, and D. Sarkar, "Refractories for Iron and Steel Plant," *Introduction to Refractories for Iron-and Steelmaking,* pp. 1-97, 2020.

[3] F. Cardarelli and F. Cardarelli, "Ceramics, refractories, and glasses," *Materials Handbook: A Concise Desktop Reference,* pp. 883-1012, 2018.

[4] P. Sengupta and I. Manna, "Advanced high-temperature structural materials in petrochemical, metallurgical, power, and aerospace sectors—An overview," *Future landscape of structural materials in India,* pp. 79-131, 2022. http://dx.doi.org/10.1007/978-981-16-8523-1_5

[5] M. A. Deneen and A. C. Gross, "Refractory materials: The global market, the global industry," *Business Economics,* vol. 45, pp. 288-295, 2010.

[6] J. Briggs, "The refractories industry-A review," *Materials Technology,* vol. 20, pp. 225-232, 2005.

[7] J. G. P. da Fonseca, "Refractory Ceramics in the Context of the Fabrication of Rocket Nozzles: Conventional Alumina and Industrial Waste Alumina-Silicate Refractory Compositions," Universidade da Beira Interior (Portugal), 2023.

[8] A. Garshin, V. Kulik, S. Matveev, and A. Nilov, "Contemporary technology for preparing fiber-reinforced composite materials with a ceramic refractory matrix," *Refractories and Industrial Ceramics,* vol. 58, pp. 148-161, 2017. https://doi.org/10.1007/S11148-017-0073-4

[9] C. Sadik, I.-E. El Amrani, and A. Albizane, "Recent advances in silica-alumina refractory: A review," *Journal of Asian Ceramic Societies,* vol. 2, pp. 83-96, 2014. https://doi.org/10.1016/j.jascer.2014.03.001

[10] A. Ghosh, S. Sinhamahapatra, and H. S. Tripathi, "Refractories as advanced structural materials for high temperature processing industries," *Future Landscape of Structural Materials in India,* pp. 279-292, 2022. http://dx.doi.org/10.1007/978-981-16-8523-1_11

[11] K. Dana, S. Sinhamahapatra, H. S. Tripathi, and A. Ghosh, "Refractories of alumina-silica system," *Transactions of the Indian Ceramic Society,* vol. 73, pp. 1-13, 2014. http://dx.doi.org/10.1080/0371750X.2014.905265

[12] K. S. Randhawa, "A state-of-the-art review on advanced ceramic materials: fabrication, characteristics, applications, and wettability," *Pigment & Resin Technology,* 2023. https://doi.org/10.1108/PRT-12-2022-0144

[13] M. F. Zawrah, M. A. Taha, and R. A. Youness, "Advanced ceramics: Stages of development," in *Advanced Ceramics*, ed: Springer, 2023, pp. 1-46. https://doi.org/10.1007/978-3-031-43918-6_1

[14] N. B. Dahotre, P. Kadolkar, and S. Shah, "Refractory ceramic coatings: processes, systems and wettability/adhesion," *Surface and Interface Analysis: An International Journal devoted to the development and application of techniques for the analysis of surfaces, interfaces and thin films,* vol. 31, pp. 659-672, 2001. https://doi.org/10.1002/SIA.1092

[15] J. Binner, M. Porter, B. Baker, J. Zou, V. Venkatachalam, V. R. Diaz*, et al.*, "Selection, processing, properties and applications of ultra-high temperature ceramic matrix composites, UHTCMCs–a review," *International Materials Reviews,* vol. 65, pp. 389-444, 2020. https://doi.org/10.1080/09506608.2019.1652006

[16] R. Phiri, S. M. Rangappa, S. Siengchin, O. P. Oladijo, and T. Ozbakkaloglu, "Advances in Lightweight Composite Structures and Manufacturing Technologies: A Comprehensive Review," *Heliyon,* 2024. http://dx.doi.org/10.1016/j.heliyon.2024.e39661

[17] S. Kamara, W. Wang, and C. Ai, "Fabrication of Refractory Materials from Coal Fly Ash, Commercially Purified Kaolin, and Alumina Powders," *Materials,* vol. 13, p. 3406, 2020. https://doi.org/10.3390/ma13153406

[18] P. J. Sánchez-Soto, D. Eliche-Quesada, S. Martínez-Martínez, L. Pérez-Villarejo, and E. Garzón, "Study of a waste kaolin as raw material for mullite ceramics and mullite refractories by reaction sintering," *Materials,* vol. 15, p. 583, 2022. https://doi.org/10.3390/ma15020583

[19] P. V. López, M. F. Hernández, A. Mocciaro, D. Richard, and N. M. Rendtorff, "MoO3 and AlF3 effect on the properties of porous mullite ceramics with needle-like microstructure," *International Journal of Applied Ceramic Technology,* p. e14947, 2024. http://dx.doi.org/10.1111/ijac.14947

[20] L. Sun, Z. Wang, and B. Gao, "Ceramic membranes originated from cost-effective and abundant natural minerals and industrial wastes for broad applications—A review," *Desalin. Water Treat,* vol. 201, pp. 121-138, 2020. https://doi.org/10.5004/dwt.2020.25910

[21] I. Ganesh and J. M. Ferreira, "Influence of raw material type and of the overall chemical composition on phase formation and sintered microstructure of mullite aggregates," *Ceramics International,* vol. 35, pp. 2007-2015, 2009. https://doi.org/10.1016/j.ceramint.2008.11.008

[22] L. Lima, K. Silva, R. Menezes, L. Santana, and H. Lira, "Microstructural characteristics, properties, synthesis and applications of mullite: a review," *Cerâmica,* vol. 68, pp. 126-142, 2022. http://dx.doi.org/10.1590/0366-69132022683853184

[23] F. Findik, "Review of high temperature materials," *Heritage and Sustainable Development,* vol. 5, pp. 213-228, 2023. http://dx.doi.org/10.37868/hsd.v5i2.163

[24] R. Sarkar, "Nanotechnology in refractory castables—an overview," *Interceram-International Ceramic Review,* vol. 67, pp. 22-31, 2018. https://doi.org/10.1007/s42411-018-0039-7

[25] L. Zhuo, Y. Xie, and B. Chen, "A review on recent progress of refractory high entropy alloys: From fundamental research to engineering applications," *Journal of Materials Research and Technology,* 2024. https://doi.org/10.1016/j.jmrt.2024.09.131

[26] M. I. Boulos, P. L. Fauchais, J. V. Heberlein, M. I. Boulos, P. L. Fauchais, and J. V. Heberlein, "Industrial applications of thermal spray technology," *Thermal Spray Fundamentals: From Powder to Part,* pp. 997-1096, 2021. http://dx.doi.org/10.1007/978-3-030-70672-2_19

[27] J. Ye, "Preparation and Characterisation of Novel Carbon Materials for Refractory Castable Applications," University of Sheffield, 2014. https://etheses.whiterose.ac.uk/id/oai_id/oai:etheses.whiterose.ac.uk:5654

[28] V. Antonovič, J. Szczerba, J. Keriene, R. Stonys, and R. Boris, "Refractory materials for biofuel boilers," *Frontiers in Bioenergy and Biofuels,* vol. 443, 2017. http://dx.doi.org/10.5772/65550

[29] V. Antonovič, R. Stonys, R. Boris, and J. Malaiškienė, "Effect of quartz sand on the properties and alkali resistance of refractory aluminosilicate castables," *Construction and Building Materials,* vol. 351, p. 128978, 2022. http://dx.doi.org/10.1016/j.conbuildmat.2022.128978

[30] M. R. Abdullah and Z. Peng, "Review and perspective on additive manufacturing of refractory high entropy alloys," *Materials Today Advances,* vol. 22, p. 100497, 2024. http://dx.doi.org/10.1016/j.mtadv.2024.100497

[31] H. Zuo, W. Wei, Z. Yang, X. Li, J. Ren, Y. Xian*, et al.*, "Performance enhancement of carbon/copper composites based on boron doping," *Journal of Alloys and Compounds,* vol. 876, p. 160213, 2021. http://dx.doi.org/10.1016/j.jallcom.2021.160213

[32] J. Meng, J. Huang, and X. Xu, "Thermophysical properties of Cu-coated carbon fibers reinforced aluminum matrix composites by stir casting," *Carbon Letters,* vol. 33, pp. 2053-2061, 2023. http://doi.org/10.1007/s42823-023-00555-7

[33] W. Wei, Z. Huang, G. Yin, Z. Yang, X. Li, H. Zuo*, et al.*, "Thermal shock resistance enhancement by improved interfacial bonding for carbon/aluminium composites," *High Voltage,* vol. 7, pp. 960-967, 2022. http://dx.doi.org/10.1049/hve2.12190

[34] Y. Li, Z. Huang, L. Dong, X. Liu, G. Yuan, H. Lei*, et al.*, "Carbon nanotubes-functionalized MgO-based castables: Super-nonwetting behavior and slag corrosion resistance," *Construction and Building Materials,* vol. 442, p. 137601, 2024.

[35] C. Strąk, W. Olesińska, and R. Siedlec, "Influence of carbon and oxygen on properties of Cu-CO composites," *Materiały Elektroniczne,* vol. 44, pp. 7--19, 2016.

[36] A. Luz, R. Salomão, C. Bitencourt, C. Renda, A. Lucas, C. Aneziris*, et al.*, "Thermosetting resins for carbon-containing refractories: theoretical basis and novel insights," *Open Ceramics,* vol. 3, p. 100025, 2020. https://doi.org/10.1016/j.oceram.2020.100025

[37] V. Muñoz, P. Pena, and A. G. T. Martínez, "Physical, chemical and thermal characterization of alumina–magnesia–carbon refractories," *Ceramics International,* vol. 40, pp. 9133-9149, 2014. https://doi.org/10.1016/j.ceramint.2014.01.128

[38] P. Suhasinee Behera and S. Bhattacharyya, "Sintering and microstructural study of mullite prepared from kaolinite and reactive alumina: effect of MgO and TiO2," *International Journal of Applied Ceramic Technology,* vol. 18, pp. 81-90, 2021. https://doi.org/10.1111/ijac.13637

[39] N. Sadli, A. May, M. Hamidouche, A. Henniche, H. Belhouchet, and H. Boudouh, "Investigations on kaolin mixtures: Impact on mullite formation kinetics and microstructure evolution," *International Journal of Applied Ceramic Technology,* 2024. http://dx.doi.org/10.1111/ijac.14820

[40] T. Sahraoui, H. Belhouchet, M. Heraiz, N. Brihi, and A. Guermat, "The effects of mechanical activation on the sintering of mullite produced from kaolin and aluminum powder," *Ceramics International,* vol. 42, pp. 12185-12193, 2016. https://doi.org/10.1016/j.ceramint.2016.04.157

[41] V. Viswabaskaran, F. Gnanam, and M. Balasubramanian, "Mullitisation behaviour of calcined clay–alumina mixtures," *Ceramics International,* vol. 29, pp. 561-571, 2003. http://dx.doi.org/10.1016/S0272-8842(02)00203-1

[42] D. Soumya, "Processing of Mullite based Ceramics Using Bauxite-Fly ash Mixture," 2015. https://api.core.ac.uk/oai/oai:generic.eprints.org:6933/core1451

[43] I. A. Aksay, D. M. Dabbs, and M. Sarikaya, "Mullite for structural, electronic, and optical applications," *Journal of the American Ceramic Society,* vol. 74, pp. 2343-2358, 1991. https://doi.org/10.1111/j.1151-2916.1991.tb06768.x

[44] M. D. Johnston, L. T. Khajavi, M. Li, S. Sokhanvaran, and M. Barati, "High-temperature refining of metallurgical-grade silicon: A review," *Jom,* vol. 64, pp. 935-945, 2012. http://dx.doi.org/10.1007/s11837-012-0384-3

[45] I. J. Fernandes, D. Calheiro, F. A. Sánchez, A. L. D. Camacho, T. L. A. d. C. Rocha, C. A. M. Moraes, *et al.*, "Characterization of silica produced from rice husk ash: comparison of purification and processing methods," *Materials Research,* vol. 20, pp. 512-518, 2017. http://dx.doi.org/10.1590/1980-5373-mr-2016-1043

[46] N. Soltani, A. Bahrami, M. Pech-Canul, and L. González, "Review on the physicochemical treatments of rice husk for production of advanced materials," *Chemical engineering journal,* vol. 264, pp. 899-935, 2015. https://doi.org/10.1016/j.cej.2014.11.056

[47] B. Thethwayo and J. Steenkamp, "A review of carbon-based refractory materials and their applications," *Journal of the Southern African Institute of Mining and Metallurgy,* vol. 120, pp. 641-650, 2020. http://dx.doi.org/10.17159/2411-9717/1011/2020

[48] E. M. M. Ewais, "Carbon based refractories," *Journal of the Ceramic Society of Japan (日本セラミックス協会学術論文誌),* vol. 112, pp. 517-532, 2004. https://doi.org/10.1016/j.ceramint.2020.05.153

[49] E.-W. Jacobs, "Fused Alumina-Pure and Alloyed--as an Abrasive and Refractory Material," *Alumina chemicals: science and technology handbook,* p. 393, 1990.

[50] S. Nanda, A. Choudhury, K. S. Chandra, and D. Sarkar, "Raw materials, microstructure, and properties of MgO–C refractories: directions for refractory recipe development," *Journal of the European Ceramic Society,* vol. 43, pp. 14-36, 2023.

[51] R. Moreno, "Better ceramics through colloid chemistry," *Journal of the European Ceramic Society,* vol. 40, pp. 559-587, 2020. https://doi.org/10.1016/j.jeurceramsoc.2019.10.014

[52] R. Singh, "Mullite Ceramic from Diphasic Precursor Powder," 2016.

[53] V. K. Atanga, "Processing and properties of alumina reinforced mullite ceramics," Universitätsbibliothek, 2013.